Molecular Crystals and Liquid Crystals

Publication details, including instructions for authors and subscription information:
http://www.tandfonline.com/loi/gmcl20

CHARACTERIZATION OF MICRON AND SUBMICRON SCALE LATERAL STRUCTURE OF OPTICALLY NONLINEAR ORGANIC FILMS

I. A. Maslyanitsyn [a], V. D. Shigorin [a], L. Todorova [b], Y. Marinov [b] & A. G. Petrov [b]

[a] General Physics Institute of Russian Academy of Sciences, 38 Vavilov str., 117942 Moscow, Russia

[b] Institute of Solid State Physics, 72 Tzarigradsko Chaussee Blvd., 1784 Sofia, Bulgaria

Version of record first published: 15 Jul 2010

To cite this article: I. A. Maslyanitsyn, V. D. Shigorin, L. Todorova, Y. Marinov & A. G. Petrov (2004): CHARACTERIZATION OF MICRON AND SUBMICRON SCALE LATERAL STRUCTURE OF OPTICALLY NONLINEAR ORGANIC FILMS, Molecular Crystals and Liquid Crystals, 408:1, 71-81

To link to this article: http://dx.doi.org/10.1080/15421400490425900

Mol. Cryst. Liq. Cryst., Vol. 408, pp. 71–81, 2004

ISSN: 1542-1406 print/1563-5287 online
DOI: 10.1080/15421400490425900

Taylor & Francis
Taylor & Francis Group

CHARACTERIZATION OF MICRON AND SUBMICRON SCALE LATERAL STRUCTURE OF OPTICALLY NONLINEAR ORGANIC FILMS

I. A. Maslyanitsyn and V. D. Shigorin
General Physics Institute of Russian Academy of Sciences, 38 Vavilov str., 117942 Moscow, Russia

L. Todorova, Y. Marinov, and A. G. Petrov
Institute of Solid State Physics, 72 Tzarigradsko Chaussee Blvd., 1784 Sofia, Bulgaria

Second harmonic generation, optical microscopy, and atomic force microscopy (AFM) are used for the investigation of the thin films of azobenzene and transstilbene derivatives. Film morphology is studied at micron and submicron scale. The approach allows one to estimate the size and internal ordering of the crystalline molecular aggregates. The effect of the dilution with stearic acid is discussed.

Keywords: second harmonic generation; film morphology

INTRODUCTION

Organic films are believed to be perspective materials for optoelectronics [1]. Low cost and relatively flexible fabrication process is an important advantage of these films. However, the problems of the film degradation are not solved to date. The films have been extensively studied last decade but the problem still remains, and interest in the stable crystalline forms of organic materials is growing [2–4]. Therefore, the investigation of the film

This investigation was carried out in the framework of the activity of Bulgarian-Russian interacademical exchange program (project "New perspective materials for electronics on the base of thin organic films") and the Joint Orientationally Ordered Media Laboratory (OOM-Lab) and was partially supported by the European Community in the frame of the INCO Copernicus Concerted Action "Photocom" under Contract No. IC15-CT98-0806. The authors acknowledge Dr. N. K. Tolochko for the synthesis of CMONS and BONS and the chemists of OOM-Lab /NIOPIK for the synthesis of ACAB.

Corresponding author. E-mail: maslian@ran.gpi.ru

morphology is actual. For example, a number of optical methods was used for the investigation of the films. Formation of two-dimensional crystalline structures of cyanide dye on the water surface was investigated with fluorescence microscopy [5]. If the film possesses lowest order optical nonlinearity, one can use second harmonic generation (SHG). The films of 2-docosylamino-5-nitropyradine (DCANP) were characterized using second harmonic (SH) microscopy [6]. The morphology of 2-methyl-4-nitroaniline (MNA) crystalline films and induced spatial modulation of optical nonlinearities in the films of oriented Disperse Red 1 (DR1); PMMA electrooptic polymers were investigated using reflectance SH technique [7]. The resolution of these methods is limited with either diffraction effect or beam focus diameter and is usually equal to some microns. It was proposed earlier [8] to use a dependence of transmitted SH intensity on pump incidence angle for the micron and submicron scale estimation of lateral size of the film domains with acentric molecular ordering. Multilayer Langmuir-Blodgett (LB) films of a number of azobenzene derivatives were investigated, and two types of the SH dependence on pump incidence angle were observed. It was suggested that the effect is governed by the ratio of average domain size r to the SH wavelength λ. However, there were no additional experiments involving the direct observation of such domains that usually are crystalline molecular aggregates or, simply, crystallites.

In this article we investigated the morphology of some organic films using SHG method as well as the direct ones: polarization optical microscopy and atomic force microscopy (AFM).

EXPERIMENTAL METHODS

The films of β-cyano-4-methoxy-4′- nitrostilbene (CMONS), 4-bromo-4′-nitrostilbene (BONS) [9,10], and 4-cyano-4′-N-hexadecylaminoazobenzene (ACAB) in pure form and in mixture with stearic acid were investigated. Structural formula of the studied compounds are shown in Figure 1.

Both BONS and CMONS demonstrated significant aggregation in solutions [9]. For this reason the compounds were intentionally used to produce isolated crystalline domains (microcrystals). It was possible to observe such structures and identify the crystallites both with optical microscope and AFM. To analyze the effect of bulk substituent another compound, ACAB, was studied. LB trough KSV 5000 was used in our experiments, and a process of spontaneous crystallization took place on water surface. Pure compounds were spread onto aqueous subphase from 10^{-3} M chloroform solution. Since the films of pure compounds did not sustain high lateral pressure and demonstrated significant aggregation, the films were compressed to relatively low surface pressures in the range of

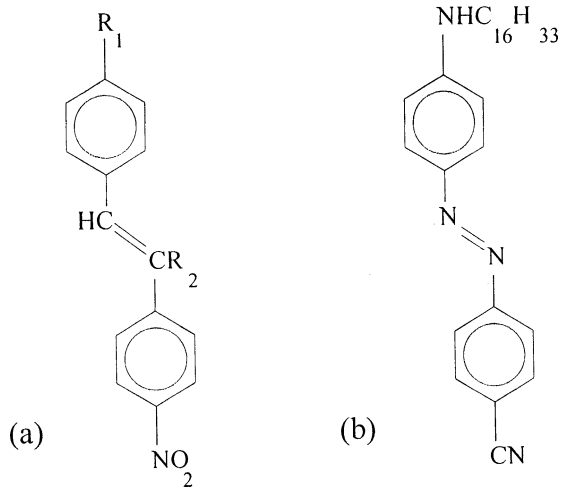

FIGURE 1 Structural formula of the investigated molecules. (a) CMONS (R_1 = OCH_3, R_2 = CN) and BONS (R_1 = Br, R_2 = H); (b) ACAB.

1–3 mN/m before the deposition. The calculated areas per molecule were 0.055, 0.045, and 0.14 nm^2 for BONS, CMONS, and ACAB, respectively. Mixtures of the investigated compounds with stearic acid (mole ratio 1:3) were dissolved in chloroform so that the concentration of optically nonlinear compound was $0.25 \cdot 10^{-3}$ M. The respective isotherms are shown in Figure 2. The films of BONS mixture were compressed to 10 mN/m before the deposition, and respective pressure value for CMONS and ACAB mixtures was 30 mN/m. Both pure and mixed films were transferred onto hydrophilic glass substrates from the surface of aqueous subphase (20°C, pH = 6.6) by vertical lift method.

Experimental SHG setup is shown in Figure 3. Pump source was Q-switched Nd^{3+}: YAG laser with wavelength 1064 nm pulse duration 30 ns, and pulse energy 5 mJ. The beam was focused on the sample to 1 mm diameter spot. SHG origin of the signal was checked by quadratic dependence of its amplitude on pump intensity. The quality of the deposition was verified using two-dimensional laser beam scanning of the sample surface (step 1 mm, pump incidence angle 45°). Then the dependencies of transmitted SH intensity on incidence angle of pump beam were measured for selected films. Pump waves, as well as analyzed SH waves, were p-polarized in all experiments. Only samples coated on one side were used in our experiments.

Polarization microscopy measurements were carried out using Carl Zeiss Universal Research Microscope Nu-2 combined with a color video camera (Hitachi VK-C150ED). Film morphology was studied in polarizing

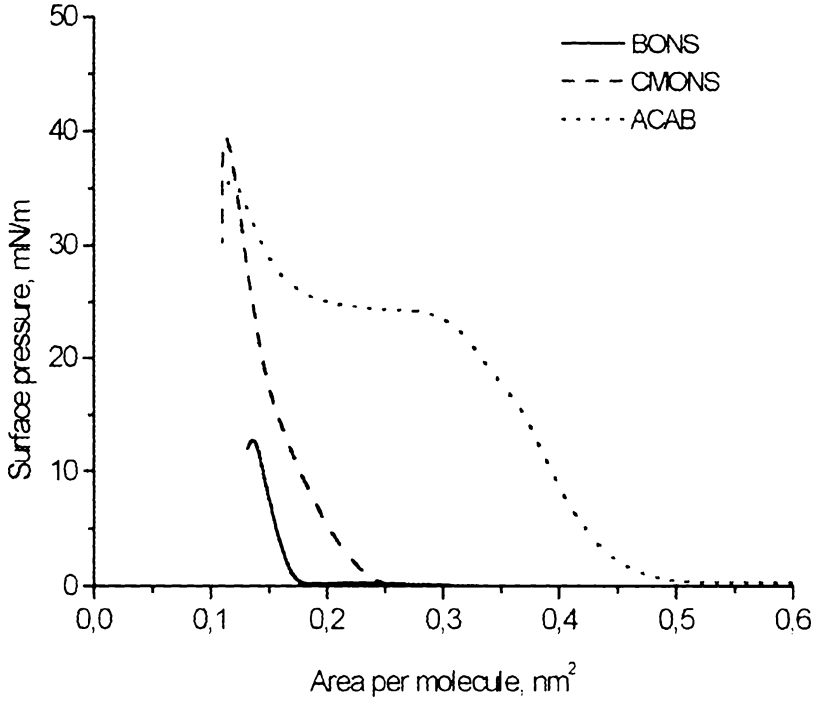

FIGURE 2 Pressure-area isotherms for the mixtures of the investigated compounds with stearic acid.

microscope mode between crossed nicols, in reflected or ortoscopic regime in white light. Video-recording registration was used. Additional investigation of the film morphology was carried out using atomic force microscope P-4 (NT MDT, Russia) in constant contact mode.

RESULTS AND DISCUSSION

SHG during two-dimensional laser beam scanning of the sample surface revealed good homogeneity of both pure and mixed samples of BONS and ACAB, whereas CMONS films (pure compound and mixture) demonstrated some inhomogeneity. The experiments, when the samples were rotated around various axes lying in the substrate plane, indicated ∞m symmetry of the pattern of transmitted SH intensity $I(\theta_i, \varphi_i)$ (θ_i is polar angle and φ_i is azimuthal one of the pump beam) in all cases. This result means that azimuthal distribution of crystallites in all investigated films was uniform.

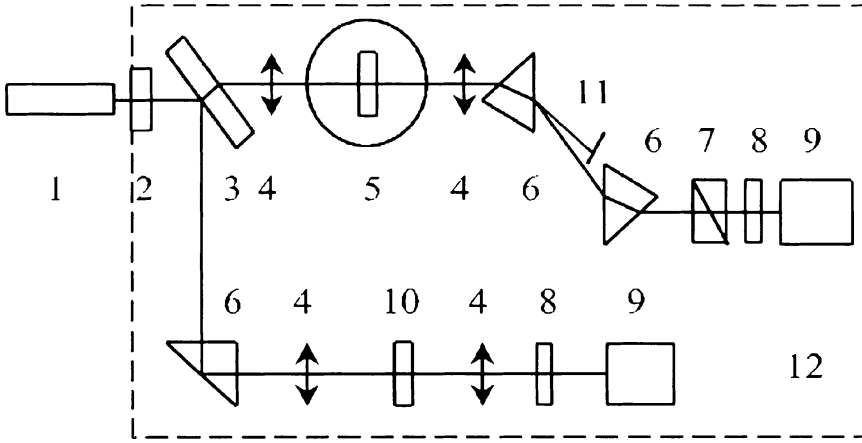

FIGURE 3 Experimental setup: (1) laser, (2) IR filter, (3) beam splitter, (4) lense, (5) stepping/rotating stage with studied sample, (6) prism, (7) analyzer, (8) SH filter, (9) photomultiplier, (10) reference α-quartz platelet, (11) screen, (12) opaque box.

Dependencies of transmitted SH intensity on the incidence angle of pump beam $I(\theta_i)$ of both pure compounds and their mixtures with stearic acid are shown in Figures 4–6.

In the case of CMONS (Figure 4) significant irregular deviations of the signal took place due to abovementioned inhomogeneities. Nevertheless, it is possible to conclude that the maximum of SH intensity occurs at the region of $\theta i = 0$. It was shown previously [8] that such a situation takes place for large crystallites ($r >> \lambda$) and a molecular tilt angle (angle between long molecular axis and surface normal) close to 90°. The theoretical curve for this case was calculated by means developed in Maslyanitsyn and Shigorin [8] model in void absence approximation and is shown in Figure 4. Micrograph of pure compound film (Figure 7(a)) confirms the existence of relatively large crystallites separated by voids. One can see bright needle-like objects randomly distributed at the sample surface. Their average length was estimated as 50 μm and the length-to-width ratio as exceeding 10. This structure of CMONS samples enabled us to use atomic force microscope. It was established in AFM experiments that pure CMONS film consists of isolated striplike crystallites with an average width of 1 μm and a height of 100 nm (Figure 8(a)). This is in agreement with the results of Tolochko et al. [9], where needle-like crystals with length up to 1 mm and thickness below 0.1 mm were observed in the process of bulk crystallization. The reduction of the crystallite size in the investigated films compared to the case of the bulk crystallization can

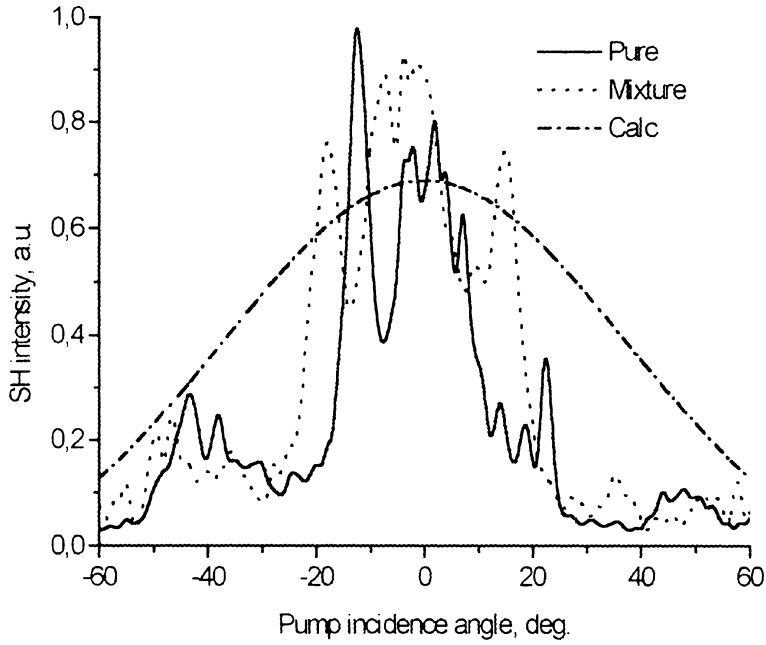

FIGURE 4 Normalized SH intensity dependencies on pump beam incidence angle for CMONS films.

account for very rapid evaporation of the solvent from the water surface. It is likely that these crystallites are microcrystals with symmetry similar to that of the bulk crystal. Their length meets the condition $r >> \lambda$.

When CMONS had been mixed with stearic acid then an unusual result was obtained: the films demonstrated the same pattern of SH intensity, whereas it was not possible to detect any heterogeneous structure using an optical microscope (Figure 7(b)). Respective AFM measurements demonstrated significant reduction of the film roughness compared to the pure compound film (Figure 8(b)). One can see also difference in the morphology of the two films. Average in-plane size of the relief inhomogeneities is less than one micron. However, the crystallites in mixed CMONS films are still capable of generating the same SH pattern as in pure compound films, i.e., $r >> \lambda$. Possible explanation of this fact is as follows. When stearic acid is added to the film then the molecules of stearic acid fill free space between CMONS crystallites and mask them both for optical and atomic force microscopes. However, nonlinear optical properties of the mixed film are similar to the pure compound film because the hyperpolarizability of stearic acid molecule is negligible compared to that of CMONS.

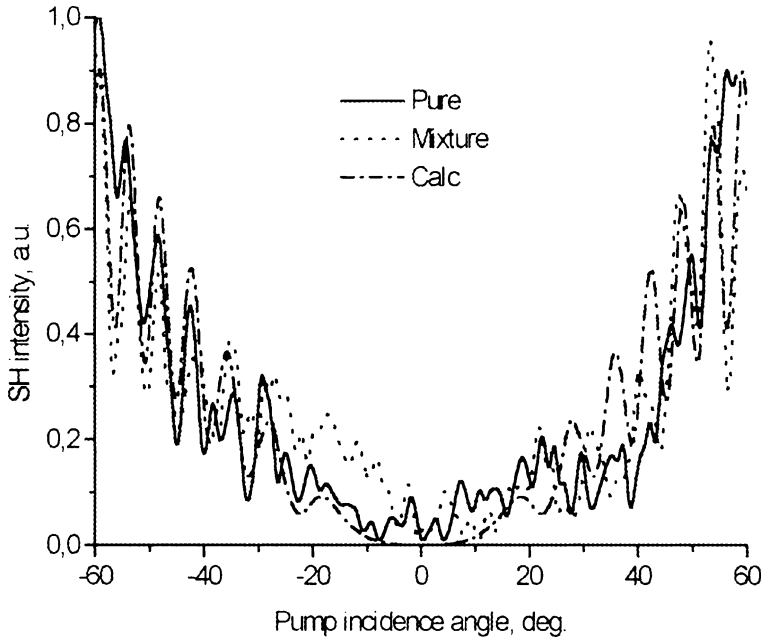

FIGURE 5 Normalized SH intensity dependencies on pump beam incidence angle for BONS films.

The films of pure BONS compound demonstrated an inhomogeneous structure (Figure 9(a)). Note that BONS particles with indefinite form and a size of 0.1 mm have been observed in Tolochko et al. [11]. In the investigated films an optical contrast of BONS aggregates was reduced compared to that of CMONS, and it was not possible to identify separate crystallites. This was the case for the respective AFM images also. Experimental and calculated SHG curves of BONS film are shown in Figure 5. Their pattern is typical for the film with small crystallites ($r << \lambda$). Conventional SHG model (see Maslyanitsyn and Shigorin [8] and references therein) was used, and one can see good agreement between calculated and experimental curves. Thus one can conclude that aggregates shown in Figure 9(a) have no internal polar ordering compared to those of CMONS. Adding stearic acid to BONS did not change the SHG pattern; only a small general reduction of the intensity was observed. Micrographs of the mixed BONS film were similar to those of Figure 7(b). AFM images showed surface with 20 nm roughness without any pronounced details.

Pure ACAB films demonstrated intermediate case ($r \cong \lambda$) of SH pattern, as depicted in Figure 6. In the micrograph (Figure 9(b)) bright aggregates

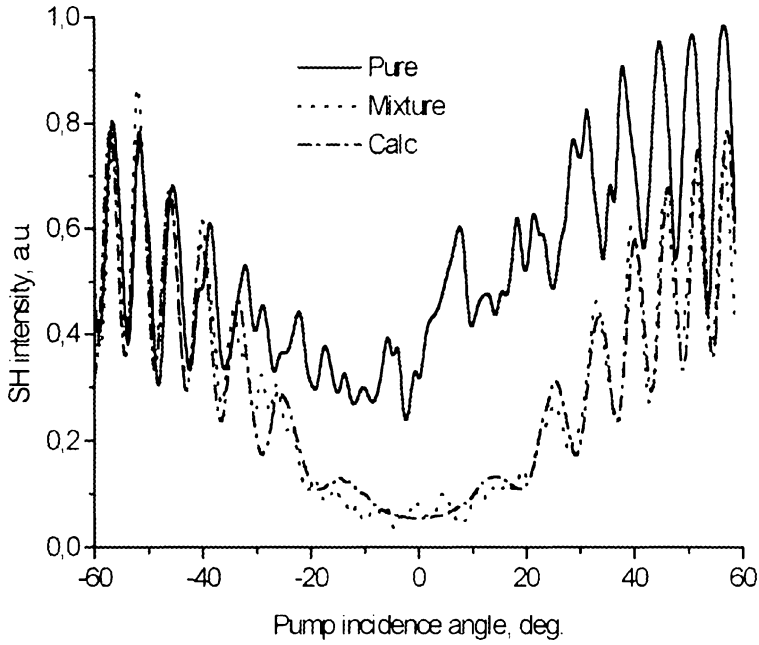

FIGURE 6 Normalized SH intensity dependencies on pump beam incidence angle for ACAB films.

of 5 μm size are observable. The same size of the aggregates with height of about 150 nm was obtained in AFM experiments (Figure 10). One can also see in this image some aggregates of small size (less than 2 μm). The contribution of these small size crystallites to the SHG can account for the

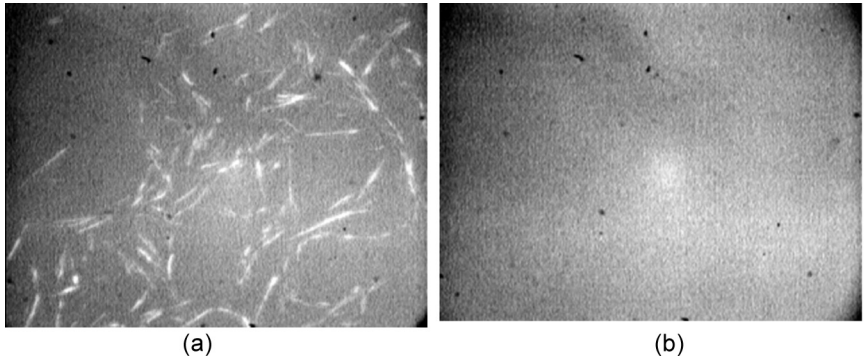

FIGURE 7 Micrographs (400 × 300 μm^2) of CMONS films: (a) pure compound; (b) mixture with stearic acid.

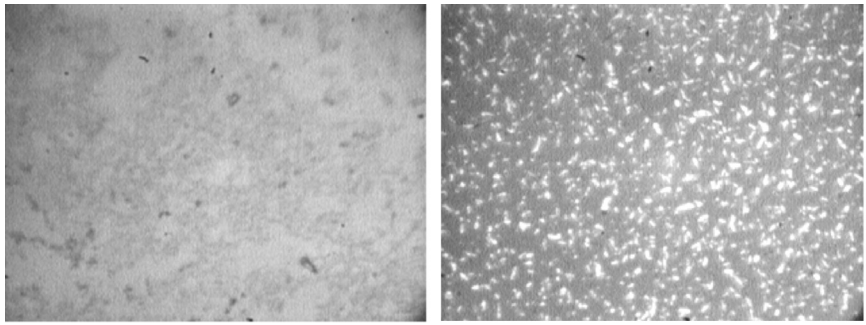

FIGURE 8 AFM images of CMONS films, $20 \times 20\,\mu m^2$: (a) pure compound; (b) mixture with stearic acid.

above-mentioned intermediate nature of the observed dependence. When stearic acid was added to the film the pattern of SH changed. The most dramatic reduction of the SH intensity (estimated from the envelope curve) was observed in the area around $\theta_i = 0$ (5 times). Thus the SH pattern of mixed ACAB film is much more similar to the pattern of small crystallite film than that of pure compound. For the fitting of the theoretical curve (see Figure 6) a combination of the two above-mentioned models was used, and the result is in good agreement with experiment.

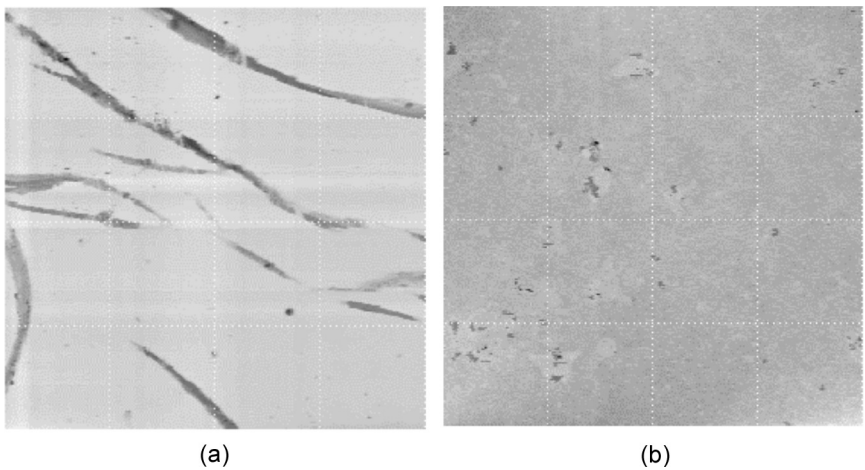

FIGURE 9 Micrographs ($400 \times 300\,\mu m^2$) of pure compound films: (a) BONS and (b) ACAB.

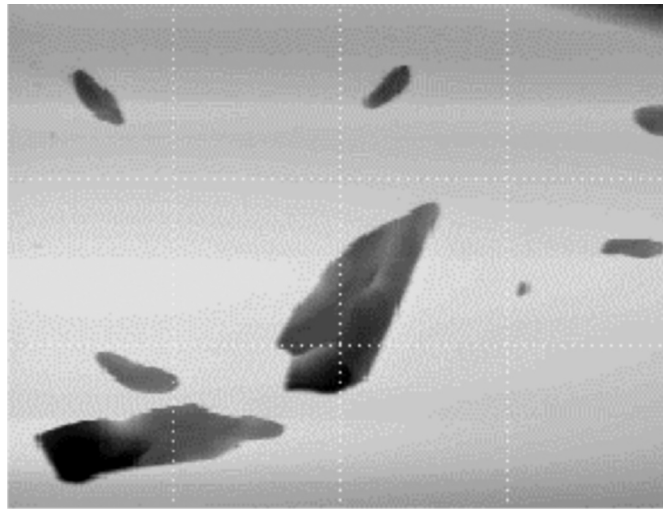

FIGURE 10 AFM image of pure ACAB film, $20 \times 15\,\mu m^2$.

Micrographs of the mixed ACAB films were similar to those in Figure 7(b), and a typical AFM image was similar to the one in Figure 8(b).

Thus, the investigations of pure compound films have revealed good correlation of average crystallite size obtained by different used methods. Micrographs and AFM images of mixed films of all compounds demonstrate structureless images (one of them is shown in Figure 7(b)), whereas SHG method is still valid to reveal film crystallite structure. It is possible to suggest that the molecules of stearic acid fill free space between optically nonlinear crystallites in the case of CMONS and ACAB, and mask both of them for optical and atomic force microscopes. Also, the addition of stearic acid can reduce crystallization rate due to spatial separation of optically nonlinear molecules. Comparison of the SH patterns of the mixed CMONS and ACAB films shows that dilution with stearic acid effectively reduces this rate in the latter case and is not effective in the former. One of the possible factors influencing the rate is that the CMONS molecule is relatively short with compact substituents, whereas ACAB has a long aliphatic tail. It is likely that the tail can interact with aliphatic tails of stearic acid molecules, resulting in the specific shape of the isotherm (see Figure 2) and reducing the rate of the crystallization.

In summary, SHG method, optical microscopy, and AFM were used for the investigation of thin films of stilbene and azobenzene derivatives. It was demonstrated that it is possible to use the SHG method to study film crystallite structures hidden for both direct methods, optical microscopy

and AFM. The proposed approach allows one to estimate average crystallite size on a micron and submicron scale, as well as angular distribution and internal ordering of crystallites. It can be used in the investigation of thin organic film morphology.

REFERENCES

[1] Khoo, I. C., Simoni, F., & Umeton, C. (Eds.) (1996). *Novel Optical Materials and Applications* (New York: Wiley).
[2] Damman, P., Vallee, R., Dosiere, M., Toussaere, E., & Zyss, J. (2001). Oriented crystallizaton NLO organic materials. *Synthetic Metals, 124*, 227–232.
[3] Vijayan, N., Ramesh Babu, R., Gopalakrishnan, R., Dhanuskodi, S., & Ramasamy, P. (2001). Growth and characterization of organic NLO crystals of semicarbazone of acetophenone. *J. Cryst. Growth 233*, 863–867.
[4] Tsunesada, F., Iwai, T., Watanabe, T., Adachi, H., Yoshimura, M., Mori, Y., & Sasaki, T. (2002). High-quality crystal growth of organic nonlinear optical crystal DAST. *J. Cryst. Growth, 237–239*, 2104–2106.
[5] Watanabe, T., Asai, K., & Ishigure, K. (1998). Control of domain structure of a cyanine dye Langmuir-Blodgett film. *Thin Solid Films, 322*, 188–193.
[6] Floersheimer, M., Busch, M., Brillert, C., Wierschem, M., & Fuchs, H. (1998). Second-harmonic imaging of surface order and symmetry. *Thin Solid Films, 327–329*, 241–246.
[7] Martin, G., Toussaere, E., Soulier, L., & Zyss, J. (2002). Reflection second harmonic generation scanning microscope. *Synthetic Metals, 127*, 105–109.
[8] Maslyanitsyn, I. A. & Shigorin, V. D., (2000). Two angular patterns of second harmonic generation in Langmuir-Blodgett films. *Thin Solid Films, 374*, 119–124.
[9] Tolochko, N. K., Sobolenko, N. V., Yadroitsev, N. V., Mozzharov, S. E., & Andreev, V. B. (1994). On the crystallization of the organic compounds BANP, BONS and CMONS from low-temperature solutions. *Crystallogr. Rep., 39*, 1036–1038.
[10] Wang, Y., Tam, W., Stevenson, S. H., Clement, R. A., & Calabrese, J. (1988). New organic nonlinear optical materials of stilbene and diphenylacethylene derivatives. *Chem. Phys. Lett., 148*, 136–141.